J Sol-Gel Sci Technol (2016) 78:531–538
DOI 10.1007/s10971-016-3985-4

ORIGINAL PAPER: NANO-STRUCTURED MATERIALS (PARTICLES, FIBERS, COLLOIDS, COMPOSITES, ETC.)

Agglomeration-free silica NPs in dry storage for PBT nanocomposite

Brigida Silvestri[1] · Aniello Costantini[1] · Vincenzo Speranza[1] · Giuseppina Luciani[1] · Francesco Branda[1] · Pietro Russo[2]

Received: 4 November 2015 / Accepted: 15 February 2016 / Published online: 1 March 2016

Abstract Dispersion of nanoparticles actually plays a key role in preparing high-performance nanocomposites. Within sol–gel procedures, the Stöber method is widely used to produce monodisperse systems of silica particles with controlled size and morphology. However, if stored as dried, the Stöber silica nanoparticles form stable agglomerates that no longer resuspend. Herein, we propose a novel straightforward methodology that overcomes the irreversible aggregation of particles, ultimately leading to a very good dispersion of the filler within the polymeric matrix without any coupling agent, even long time after their preparation. This synthesis approach has been exploited to produce PBT/SiO_2 nanocomposites, as a model system. The produced nanocomposites have been analyzed and characterized by multiple techniques proving a fine dispersion of the filler within the matrix, as well as a significant increase in both thermal and dynamic mechanical properties. The proposed strategy ensures high compatibility with current industrial compounding facilities and far-reaching implementation in the preparation of polymer nanocomposites.

Graphical Abstract

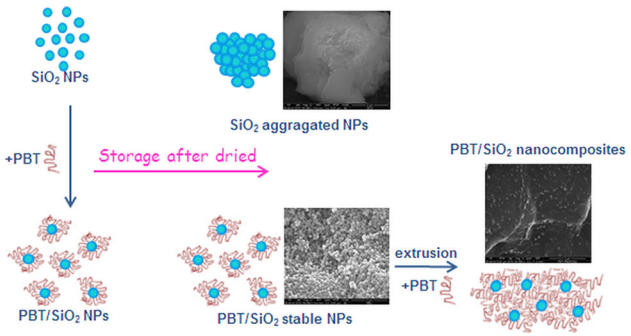

Keywords PBT/SiO_2 nanocomposites · Stöber method · Melt mixing · Agglomeration in dry storage · Thermal properties · Mechanical properties

1 Introduction

Poly(butylene terephthalate) (PBT), a well-known commercially available semicrystalline thermoplastic aromatic polyester, aroused significant attention in vast applications in automobile industry, electrical and biomedical devices [1–7].

It actually shows many valuable properties including high crystallization rate, high impact strength and thermal stability, low molding temperature, high rigidity and dimensional stability, hardness, abrasion and solvent resistance, good electrical insulation, short cycle times in injection molding, high water resistance, and good surface appearance.

Nevertheless, pure PBT has low impact strength and a heat distortion temperature. These properties can be enhanced by adding nanosized inorganic fillers such as nanoclays, silica, and carbon nanotubes into PBT matrix [8–13].

Electronic supplementary material The online version of this article (doi:10.1007/s10971-016-3985-4) contains supplementary material, which is available to authorized users.

✉ Aniello Costantini
anicosta@unina.it

[1] Department of Chemical, Materials and Production Engineering (DICMaPI), University of Naples Federico II, Piazzale Tecchio 80, 80125 Naples, Italy

[2] Institute for Polymers, Composites and Biomaterials, National Research Council, Via Campi Flegrei 34, 80078 Pozzuoli-Naples, Italy

Among those SiO_2 nanoparticles are the most preferentially used filler. They have obvious strengthening effects and thus can significantly improve both physical and mechanical properties of filled polymers [14].

Within sol–gel procedures, the Stöber method is widely used to produce silica particles due to its ability to control the particle size, size distribution, and morphology through systematic tuning of reaction parameters.

Indeed, achieving a good dispersion of nanoparticles within the matrix still remains the key challenge in this field and it is the bottleneck that limits significant improvements of nanocomposites properties.

The techniques commonly used for the production of silica–polymer nanocomposites can be categorized into three classes: solution mixing, in situ polymerization, and melt mixing processes [15, 16]. Using solvents or coupling agents [17] during solution mixing and in situ polymerization processes usually allows fine and uniform dispersion of nanoparticles, but it is not exploited because of its incompatibility with current industrial compounding facilities.

Instead, the absence of solvents makes the melt mixing process environmentally and economically sustainable, even if, for this procedure, a homogenous dispersion of nanofillers still remains a challenging aspect.

According to the universally accepted "aggregation model" [18, 19], nanometer-sized particles formed during the "nucleation" stage of sol–gel chemistry are assumed to grow solely by an aggregation process. Furthermore, interaction with macromolecules in solution can bring to an adsorbed layer and reverse the aggregation process of particles [20, 21].

However, the particles obtained using the Stöber method if dried and stored from days to week form strong interparticle bonds that lead to the formation of stable agglomerates that no longer resuspend [16, 18, 22–24]. On the other hand, avoiding the drying stage, even small amount of solvents carried out by the included particles may adversely affect the performances of the final compounds. Therefore, in order to prevent the formation of irreversible aggregates, herein, we propose a novel straightforward methodology, whereby Stöber SiO_2 nanoparticles [25] are mixed with PBT soon after their synthesis, to produce PBT-SiO_2 blends at high filler content.

The PBT shell prevents particles aggregation, making them stable during time and adaptable to be stored and then used even months after their synthesis.

Nanocomposites were characterized by multiple techniques. In detail, morphology and dispersion of the filler were assessed through scanning electron microscopy (SEM).

Thermal parameters as the glass transition temperature, the melting and the crystallization temperature as well as the degree of crystallinity were driven from differential scanning calorimetry (DSC). Thermogravimetric analysis (TGA) provided information of thermal stability and the amount of silica within the samples. Moreover, dynamic mechanical analysis (DMA) provided information on viscoelastic properties (storage modulus and mechanical loss factor).

We proved that PBT not only prevents particles aggregation, but also actually acts as an endogenous coupling agent ensuring affinity between the phases, through hydrogen bonds.

The proposed methodology actually works as an effective strategy that can overcome the major drawback of particles irreversible aggregation, ultimately leading to a very good dispersion of the filler within the polymeric matrix. Furthermore, it is highly compatible with current industrial compounding facilities and it ensures a far-reaching implementation in the preparation of polymer nanocomposites.

2 Experimental section

2.1 Materials

Poly(butylene terephthalate) (PBT) Pocan B 1505 was supplied by Lanxess GmbH (matrix). Ethanol was supplied by Fluka, Milan, Italy. Tetraethoxysilane (TEOS), ammonium hydroxide, and trifluoroacetic acid were purchased from Sigma-Aldrich, Milan, Italy, and used as received.

2.2 Synthesis of samples

Silica gel nanoparticles (SiO_2 NPs) were produced through the Stöber method [25]. Appropriate amounts of TEOS, ammonia, and water were added to ethanol; the concentrations of the obtained solution were 0.170 M TEOS, 1.0 M NH_3, and 2.0 M H_2O. The system was kept at room temperature under magnetic stirring for 2 h, and the produced particles were obtained by centrifugation and repeated washing (3 times at 12,000 rpm with distilled water). Then, an appropriate amount of the obtained wet precipitate was resuspended in a solution of PBT dissolved in trifluoroacetic acid, in order to have a 40 % w/w of silica gel nanoparticles into the final PBT-SiO_2 mixture. The mixture was dried overnight at 50 °C under vacuum, and the obtained dried powders will be indicated in the following as premixed-PBT/SiO_2 NPs.

Nanocomposites were prepared using a mini twin-screw extruder (DSM Xplore), under nitrogen, at 245 °C and a screw speed of 120 rpm, for 3 min.

Both dried SiO_2 nanoparticles, used soon after their synthesis, and dried premixed-PBT/SiO_2 nanoparticles were incorporated in pure PBT to obtain a final concentration of 3.0 wt% in silica nanoparticles. They will be indicated as PBT/SiO_2 NCs and premixed-PBT/SiO_2 NCs, respectively.

Furthermore, both SiO_2 and premixed-PBT/SiO_2 nanoparticles were stored at room temperature for 5 months.

2.3 Physico-chemical characterization

Morphological analysis was carried out by scanning electron microscopy (SEM) using a FEI Quanta 200F microscope. All samples were gold coated before the analysis.

Fourier transform infrared (FT-IR) transmittance spectra were recorded with a Nicolet FT-IR spectrometer (Thermo Fisher) using a single-reflection attenuated total reflectance (ATR) accessory with a resolution of 4 cm^{-1} and 32 scans.

Thermogravimetric analysis was performed in a thermogravimetric apparatus, TGA Q5000 TA Instruments. Samples of pure PBT, premixed-PBT/SiO_2 NPs, PBT/SiO_2 NCs, and premixed-PBT/SiO_2 NCs were heated to 700 °C at a rate of 20 °C/min under nitrogen atmosphere. Differential scanning calorimetry (DSC) was performed using a DSC Q20 TA Instruments apparatus. Encapsulated specimens (about 10 mg) of all investigated compounds were subjected under nitrogen to the following procedure: heating between 0 and 250 °C at 10 °C/min (first run), isotherm at 250 °C for 5 min in order to remove previous thermal histories, cooling at 10°/min from 250 to 0 °C, and final reheating at the same rate from 0 to 250 °C (second run). The neat PBT matrix was taken as the reference.

In order to gain an insight into the effects of the loaded silica nanoparticles on the degree of crystallinity (χ_c) of PBT matrix, the normalized χ_c values of the samples were determined, using Eq. (1):

$$\chi_c = \frac{\Delta H_m}{\Delta H^0 \left(1 - \frac{\%\text{wt filler}}{100}\right)} \times 100 \quad (1)$$

where $\Delta H^0 = 142$ J/g is the melting enthalpy of 100 % crystalline PBT [26] and ΔH_m is the melting enthalpy of the samples, measured from DSC.

Dynamic mechanical properties were analyzed using a Triton 2000 Analyser. Dynamic mechanical spectra of 40 mm × 10 mm × 3 mm were recorded for all materials in single cantilever bending mode, at a frequency of 1 Hz and using a heating rate of 3 °C/min in the range −20–140 °C.

3 Results and discussion

3.1 Morphology and microstructure

Figure 1 shows the SEM micrographies of SiO_2 NPs observed soon after their synthesis (Fig. 1a), SiO_2 NPs (Fig. 1b), and premixed-PBT/SiO_2 NPs (Fig. 1c) both observed 5 months after their synthesis.

As shown in Fig. 1a, SiO_2 NPs appear separated and show spherical morphology with a narrow size distribution and an average diameter of 70 nm. The same nanoparticles form during time unambiguous aggregates as shown in Fig. 1b.

Figure 1c shows well-separated nanoparticles with an average size of 120 nm in diameter, larger than bare SiO_2 NPs (70 nm). The increase in size can be attributed to a deposition of a PBT layer onto the nanoparticles surface formed during the drying process. Moreover, premixed-PBT/SiO_2 nanoparticles kept both morphology and size even 5 months later their synthesis, as driven from comparison of Fig. 1c with SEM micrograph of premixed-PBT/SiO_2 NPs observed soon after their synthesis (see Online Resource, ESM 1).

As it is known, nanoparticles produced through the Stöber method are easily resuspended in an unagglomerated form as just prepared.

During the drying process, the elimination of water molecules leads to the increase in the sol concentration and creates fluid drug, which causes the particles to come closer to each other (Fig. 1b). These particles touching each other form reversible aggregates where the dominant attraction forces are van der Waals and capillary types.

In addition, at the interparticle contacts, polycondensation reactions can occur if the silanol groups are close enough to react and these reactions increase in the presence of water [16, 22–24].

Indeed, due to the high hydrophilicity of silica gel nanoparticles, even after removal of most of the water, during drying step, particles do contain residual amount of adsorbed water, which promotes polycondensation reaction in the solid state over time. The effects of these processes can be dramatic and lead to irreversible aggregates after a certain period of time.

This is confirmed by SEM micrography of SiO_2 NPs observed 5 months later their synthesis (Fig. 1b), where particles shape and morphology cannot be distinguished any longer making them not stable during time and not adaptable to be stored for later use.

The use of premixed-PBT/SiO_2 NPs as filler actually avoids the further evolution of silica nanoparticles and thus greatly improves their stability, as shown in Fig. 1c.

Furthermore, a PBT layer on the particles provides a steric barrier toward aggregation, thus allowing particles redispersion even at long times.

Micrographs of both PBT/SiO_2 (Fig. 2a) and premixed-PBT/SiO_2 (Fig. 2b) nanocomposites show a good dispersion of the filler in the polymeric matrix, confirming that silica nanoparticles incorporated just prepared as well as a PBT layer onto the nanoparticles surface, i.e., premixed-PBT/SiO_2 NPs, are needed to avoid the formation of aggregates.

Actually, comparing samples just prepared and after 5 months later their synthesis, no differences are observed into the morphology not only of premixed-PBT/SiO_2 NPs but also of premixed-PBT/SiO_2 NCs (not reported), giving further confirmation to the stability of premixed-PBT/SiO_2 nanoparticles.

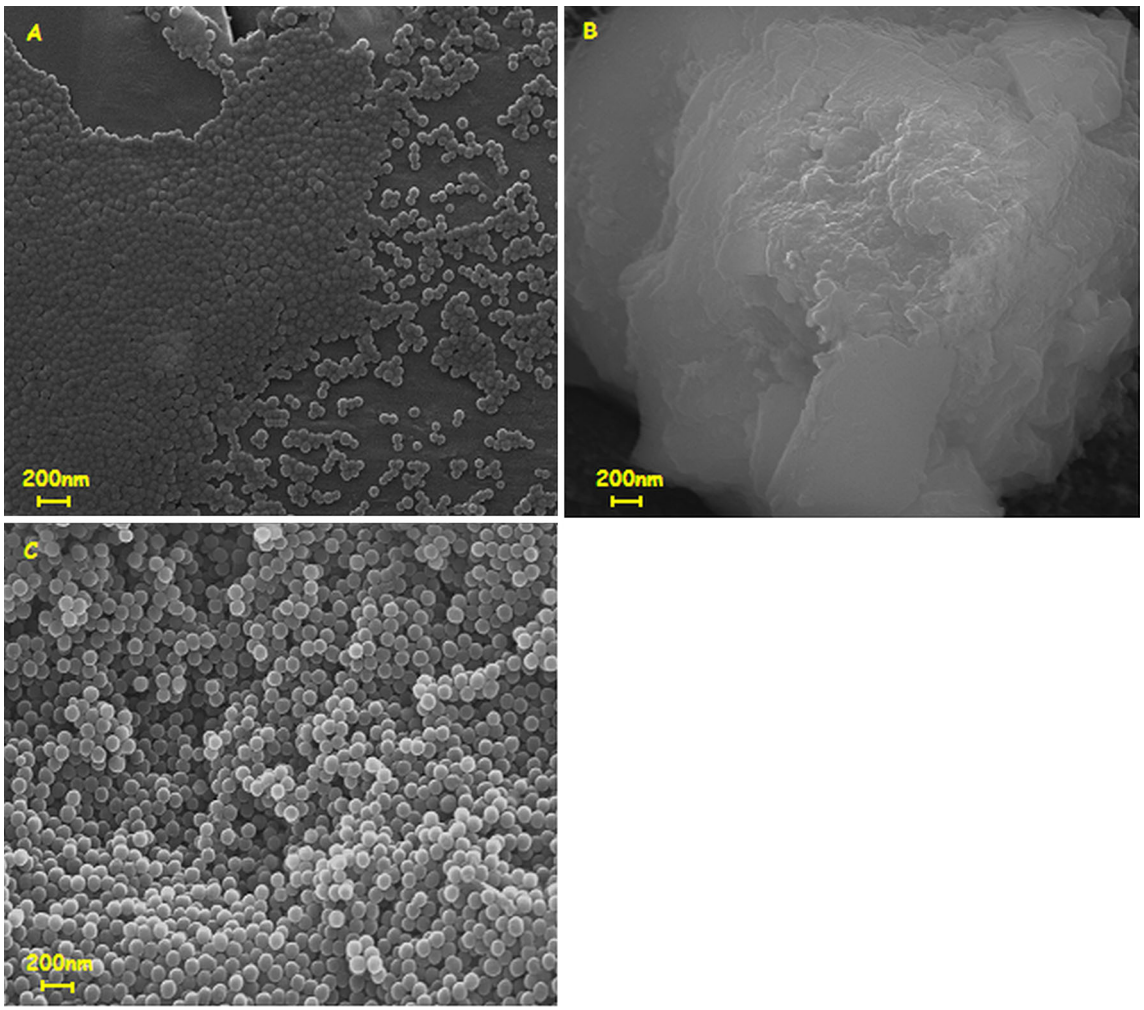

Fig. 1 SEM micrographies of just prepared SiO_2 NPs (**a**), SiO_2 NPs (**b**), and premixed-PBT/SiO_2 NPs (**c**) both 5 months after their synthesis

Figure 3 shows the FT-IR spectra of pure PBT, SiO_2 NPs, and premixed-PBT/SiO_2 NPs. As can be seen in the FT-IR spectrum of pure PBT, the most characteristic bands fall in the region between 1270 and 1710 cm^{-1} and can be assigned to C=O stretching vibration of the ester carbonyl group (1241 cm^{-1}) and to C–O stretching vibration (1098 cm^{-1}). The bands at 940, 870, and 730 cm^{-1} are related to stretching vibration of ether (C–O–C), aromatic out of plane C–H bending, and bending of the benzene rings, respectively [27, 28]. The FT-IR spectrum of SiO_2 nanoparticles shows the main characteristic bands at 1070, 950, and 800 cm^{-1} attributed to Si–O–Si stretching vibration modes in SiO_4 units, non-bridging Si–O stretching vibration, and Si–O–Si bond vibration between two adjacent tetrahedral, respectively [17, 29–31]. The bands in the spectrum of premixed-PBT/SiO_2 NPs are due to the overlapping of the main signal of both components. Moreover, a new band is visible at about 1670 cm^{-1}, in the carbonyls' stretching region (1780–1650 cm^{-1}), where both silica and PBT components show no absorption bands.

Any changes observed in this region should be directly attributed to those changes in the carbonyl group environment of PBT, such as the formation of hydrogen bonds between the hydroxyl groups of SiO_2 particles surfaces and carbonyl groups of PBT chain [32–34].

The strength of the bond considerably affects the energy of the covalent bonds on interacting species; hence, a frequency shift can be observed [32].

3.2 Thermal properties

Thermogravimetric (TG) analysis shows a weight reduction starting from about 380 °C due to the decomposition of PBT. The amount of inorganic component within the samples was 40 %w in premixed-PBT/SiO_2 NPs and 3 %w in both PBT/SiO_2 and premixed-PBT/SiO_2 nanocomposites, as driven

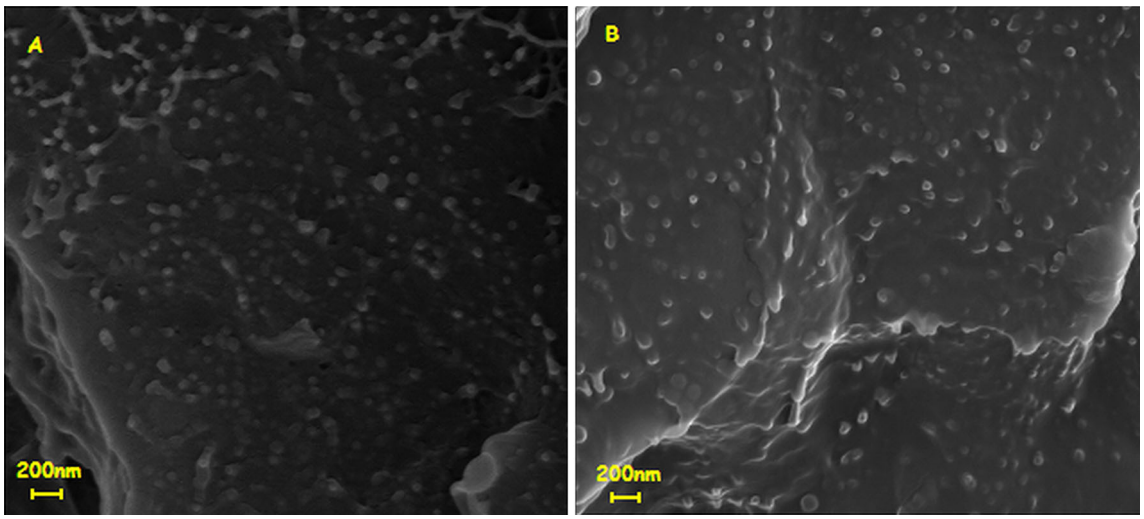

Fig. 2 SEM micrographs of PBT/SiO_2 NCs (**a**) and premixed-PBT/SiO_2 NCs (**b**)

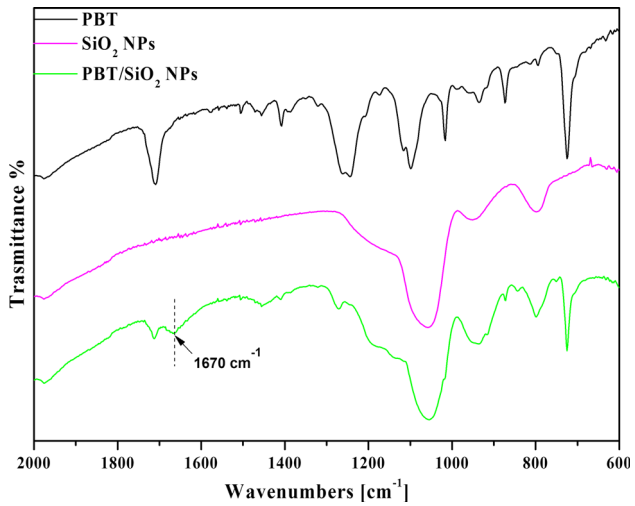

Fig. 3 FT-IR spectra of pure PBT, SiO_2 NPs and premixed-PBT/SiO_2 NPs

from residual weight at 700 °C in TG curves (see Online Resource, ESM 2).

Figure 4a shows the DSC curves of second heating of pure PBT, PBT/SiO_2 NCs, and premixed-PBT/SiO_2 NCs, while Fig. 4b shows the DSC curve recorded on cooling of premixed-PBT/SiO_2 NCs and representative of those obtained for the other samples (see Online Resource, ESM 3).

All data derived from the thermal analysis of samples are summarized in Table 1.

In particular, with regard to the melting region, a splitting of the signal is observed for the neat matrix and for the composite formulation prepared by mixing the matrix and SiO_2 particles, whereas a single peak with a slight shoulder on the left side appears in case of composites prepared by dilution of the premixed sample. The former behavior, first observed for PBT by Hobbs and Pratt [35], is generally explained assuming melting and recrystallization of thin, unstable crystals during the calorimetric scan followed by melting of more perfect crystals [36, 37].

In case of nanocomposites, it is probable that this complex fusion behavior is affected by the achieved filler distribution. An improvement of this aspect, while not promoting effect of nucleation, at least under the used operative conditions, may limit the organization of polymer macromolecules in small defective crystals favoring above all more larger stable crystals.

According to this consideration, a better distribution of SiO_2 nanoparticles can be assumed for nanocomposites from premixed-PBT/SiO_2 NPs.

Moreover, as shown in Table 1, there is an increase in melting enthalpy values (ΔH_m) from 21.56 J/g (pure PBT) to 41.67 J/g (PBT/SiO_2 NCs) and to 50.24 J/g (premixed-PBT/SiO_2 NCs) and an increase in crystallization enthalpy values (ΔH_c) from 22.38 J/g (pure PBT) to 44.62 J/g (PBT/SiO_2 NCs) and to 46.38 J/g (premixed-PBT/SiO_2 NCs).

Also crystallinity percentage (χ_c: evaluated using Eq. 1) shows an increase from 15.2 % (pure PBT) to 30.2 % (PBT/SiO_2 NCs) and to 36.5 % (premixed-PBT/SiO_2 NCs). These results confirm a good dispersion of the inorganic filler into the polymer matrix and the moderate interaction due to the formation of hydrogen bonds between the two components, in agreement with SEM micrographs and FT-IR spectra [38–40].

The dynamic mechanical properties of pure PBT and PBT/SiO_2 nanocomposites were studied by DMA. The temperature dependence of the loss factor (tanδ) and the bending storage modulus (E') at 1 Hz are shown in Fig. 5a, b, respectively, and the derived data are summarized in Table 2.

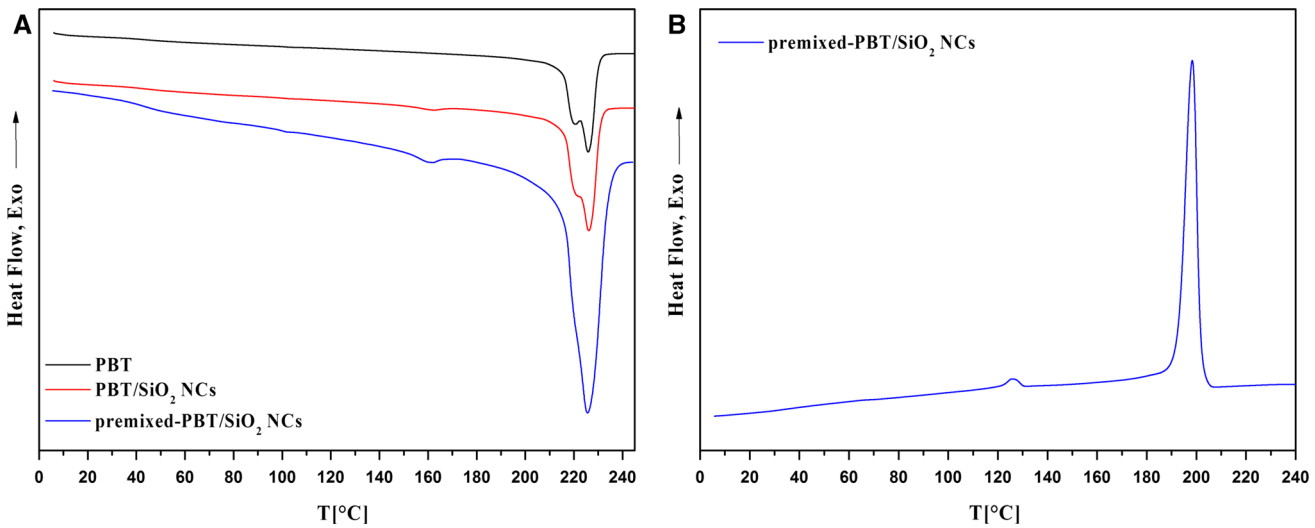

Fig. 4 DSC curves of second heating **a** of PBT, PBT/SiO_2 NCs, and premixed-PBT/SiO_2 NCs and of cooling **b** of premixed-PBT/SiO_2 NCs

Table 1 Thermal properties and crystallinity of pure PBT, PBT/SiO_2 NCs, and premixed-PBT/SiO_2 NCs

Material	T_c (°C)	ΔH_m (J/g)	ΔH_c (J/g)	χ_c (%)
PBT	199.4	21.56	22.38	15.2
PBT/SiO_2 NCs	198.9	41.7	44.62	30.2
Premixed-PBT/SiO_2 NCs	199.2	50.24	46.38	36.5

The temperature of the maximum tanδ signal, centered at about 59 °C for pure PBT and PBT/SiO_2 NCs, appears to be shifted at a higher temperature 67 °C for the premixed-PBT/SiO_2 NCs. Taking into account that this temperature is usually attributed to the glass transition temperature (T_g), the detected increase in this parameter proves again more matrix–filler interactions only possible if there is a better dispersion of the included nanoparticles in systems prepared from premixed samples.

Therefore, this result suggests that the interactions between the two phases, through hydrogen bonding confirmed by FT-IR spectra, play a fundamental role in inhibiting the polymer segmental motion.

Furthermore, the hard non-flexible silica domains could present an obstacle to random chain segment movements of the polymer matrix. This effect (different from direct interaction of the two phases) is known in literature as "topological constraint" and often could cause a T_g increase even if the phase's affinity to each other is poor [17, 41].

Finally, as clearly shown in Fig. 5a, the tanδ peak is affected particularly in terms of height. In fact, as widely established, the inclusion of rigid nanofiller gives rise to partial immobilization macromolecular chains and,

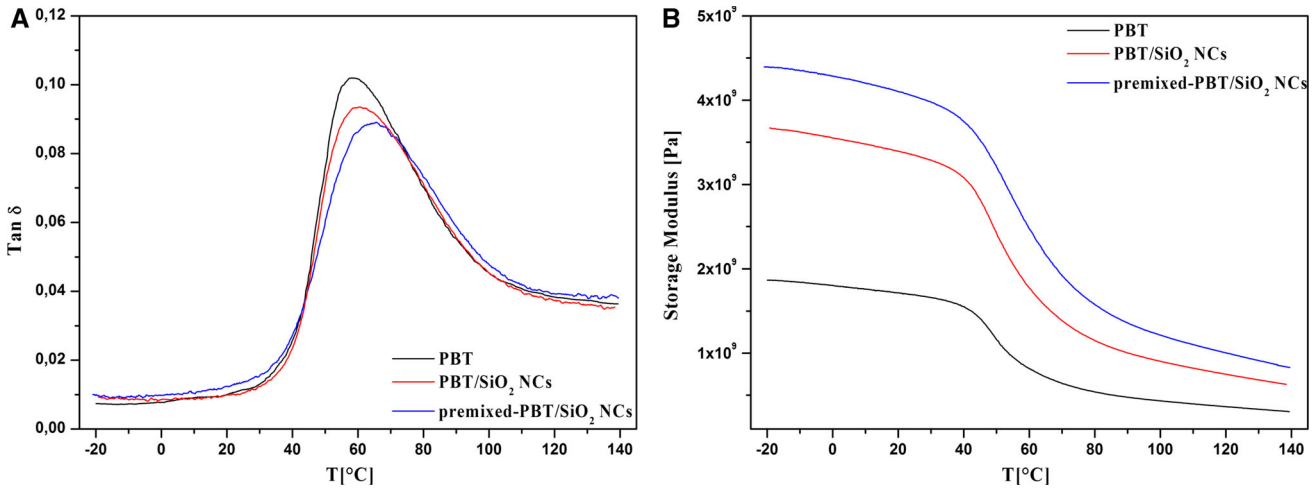

Fig. 5 DMA curves of tanδ (**a**) and E' (**b**) of PBT, PBT/SiO_2 NCs, and premixed-PBT/SiO_2 NCs

Table 2 Glass transition temperature, loss factor, and bending storage modulus of pure PBT, PBT/SiO_2 NCs, and premixed-PBT/SiO_2 NCs

Material	T_g (°C)	$E'_{-10\ °C}$ (GPa)	$E'_{120\ °C}$ (GPa)	$H_{\tan\delta,\ pk}$
PBT	58 ($\sigma = 0.91$)	1.84 ($\sigma = 0.12$)	0.37 ($\sigma = 0.061$)	0.102 ($\sigma = 0.0030$)
PBT/SiO_2 NCs	60 ($\sigma = 0.87$)	3.62 ($\sigma = 0.16$)	0.75 ($\sigma = 0.077$)	0.09 ($\sigma = 0.0032$)
Premixed-PBT/SiO_2 NCs	67 ($\sigma = 0.81$)	4.35 ($\sigma = 0.18$)	1.00 ($\sigma = 0.086$)	0.09 ($\sigma = 0.0029$)

σ SD

consequently, it reduces the mechanical damping ability of composite materials with respect to the neat hosting matrix. Considering that this effect is much more pronounced for greater matrix-filler interface, the obtained results confirm the achievement of a better dispersion of SiO_2 nanoparticles in case of premixed-PBT/SiO_2 nanocomposites.

Figure 5b shows that the E' values of PBT/silica nanocomposites are much higher than that of pure PBT over the whole temperature range with an effect more pronounced for the composite formulation obtained by diluting in PBT the premixed-PBT/SiO_2 nanoparticles. In particular, compared with pure PBT, the E' value of PBT/SiO_2 NCs increases from 1.84 to 3.62 GPa at −10 °C (97 % increase) and from 0.37 to 0.75 GPa (100 % increase) at 120 °C, respectively. Instead, increases in the premixed-PBT/SiO_2 NCs are approximately equal to 137 and 170 %, respectively. These significant improvements in E' values of PBT/silica nanocomposites are ascribed to the combined effect of the homogeneous dispersion of silica within the PBT matrix, mainly achieved using the premixed-PBT/SiO_2 nanoparticles, and the stiffening effect of the nanoparticles [13, 42].

Furthermore, these effects, particularly significant at temperatures below the glass transition temperature of the PBT, even if partly supported by the detected increase in the degree of crystallinity, suggest the occurrence of structural modifications increasing the stiffness of the amorphous phase. The finding that these modifications are not accompanied by adequate increases in the glass transition can be ascribed to the assumption that included nanoparticles may act as antiplasticizer as reported elsewhere [43].

4 Conclusions

In the present work, we proposed a successfully novel procedure to prepare PBT/SiO_2 nanocomposites with a very good dispersion of the filler within the polymeric matrix.

The use of premixed-PBT/SiO_2 filler offered the possibility to stabilize dried nanoparticles, preventing further irreversible agglomeration process making them adaptable to be stored and then used even months after their synthesis.

The significant increase in both thermal and dynamic mechanical properties of the obtained nanocomposites, compared to pure PBT, gave a further confirmation of the very good dispersion of the inorganic filler in the polymer matrix.

Experimental results proved that the affinity between the two phases was ensured by hydrogen bond between SiO_2 gel nanoparticles and PBT that actually acts as an endogenous coupling agent.

The proposed methodology is easily adaptable to different systems and compatible with current industrial compounding facilities, ensuring far-reaching implementation in the production of polymer nanocomposites.

The authors certify that they have no affiliations with or involvement in any organization or entity with any financial interest (such as honoraria; educational grants; participation in speakers' bureaus; membership, employment, consultancies, stock ownership, or other equity interest; and expert testimony or patent-licensing arrangements) or non-financial interest (such as personal or professional relationships, affiliations, knowledge, or beliefs) in the subject matter or materials discussed in this manuscript.

References

1. Sinha Ray S, Okamoto M (2003) Polymer/layered silicate nanocomposites: a review from preparation to processing. Prog Polym Sci 28:1539–1641
2. Leszczyńska A, Njuguna J, Pielichowski K, Banerjee J (2007) Polymer/montmorillonite nanocomposites with improved thermal properties: part I. Factors influencing thermal stability and mechanisms of thermal stability improvement. Thermochim Acta 453:75–96
3. Leszczyńska A, Njuguna J, Pielichowski K, Banerjee JR (2007) Polymer/montmorillonite nanocomposites with improved thermal properties: part II. Thermal stability of montmorillonite nanocomposites based on different polymeric matrixes. Thermochim Acta 454:1–22
4. Pesetskii SS, Bogdanovich SP, Myshkin NK, Fric J (2007) Tribological behavior of nanocomposites produced by the dispersion of nanofillers in polymer melts. J Frict Wear 28:457–475
5. Bhat G, Hegde RR, Kamath MG, Deshpande B (2008) Nanoclay reinforced fibers and nonwovens. J Eng Fiber Fabric 3:22–34
6. Njuguna J, Pielichowski K, Desai S (2008) Nanofiller fibre-reinforced polymer nanocomposites. Polym Adv Technol 19: 947–959
7. Hajiraissi R, Parvinzadeh M (2011) Preparation of polybutylene terephthalate/silica nanocomposites by melt compounding: evaluation of surface properties. Appl Surf Sci 257:8443–8450
8. Hong JS, Namkung H, Ahn KH, Lee SJ, Kim C (2006) The role of organically modified layered silicate in the breakup and coalescence of droplets in PBT/PE blends. Polymer 47:3967–3975

9. Xiao JF, Hu Y, Wang ZZ, Tang Y, Chen ZY, Fan WC (2005) Preparation and characterization of poly(butylene terephthalate) nanocomposites from thermally stable organic-modified montmorillonite. Eur Polym J 41:1030–1035
10. Li XC, Kang TK, Cho WJ, Lee JK, Ha CS (2001) Preparation and characterization of poly(butyleneterephthalate)/organoclay nanocomposites. Macromol Rapid Commun 22:1306–1312
11. Nogales A, Broza G, Roslaniec Z, Schulte K, Sics I, Hsiao BS, Sanz A, Garcia-Gutierrez MC, Rueda DR, Domingo C, Ezquerra TA (2004) Low percolation threshold in nanocomposites based on oxidized single wall carbon nanotubes and poly(butylene terephthalate). Macromolecules 37:7669–7672
12. Broza G, Kwiatkowska M, Roslaniec Z, Schulte K (2005) Processing and assessment of poly(butylene terephthalate) nanocomposites reinforced with oxidized single wall carbon nanotubes. Polymer 46:5860–5867
13. Zhang L, Hong Y, Zhang T, Chunzhong L (2009) A novel approach to prepare PBT nanocomposites with elastomer-modified SiO_2 particles. Polym Compos 30:673–679
14. Zhang T, Zhang L, Li C (2011) Inhibited transesterification of poly(butylene terephthalate)/poly(ethylene terephthalate)/SiO_2 nanocomposites by two processing methods. J Macromol Sci Phys 50:453–462
15. Kim D, Lee JS, Barry CMF, Mead JL (2007) Effect of fill factor and validation of characterizing the degree of mixing in polymer nanocomposites. Polym Eng Sci 47:2049–2056
16. Rahman IA, Padavettan V (2012) Synthesis of silica nanoparticles by sol–gel: size-dependent properties, surface modification and applications in silica-polymer nanocomposites: a review. J Nanomater 2012:1–15
17. Luciani G, Costantini A, Silvestri B, Tescione F, Branda F, Pezzella A (2008) Synthesis, structure and bioactivity of pHEMA/SiO_2 hybrids derived through in situ sol–gel process. J Sol–Gel Sci Technol 46:166–175
18. Bogush GH, Zukosky CF (1991) Uniform silica particle precipitation: an aggregative growth model. J Colloid Interface Sci 142:19–34
19. Lee K, Sathyagal AN, McCormick AV (1998) A closer look at an aggregation model of the Stöber process. Colloids Surf A 144:115–125
20. Branda F, Silvestri B, Costantini A, Luciani G (2015) Effect of exposure to growth media on size and surface charge of silica based Stöber nanoparticles: a DLS and ζ -potential study. J Sol–Gel Sci Technol 73:54–61
21. Branda F, Silvestri B, Costantini A, Luciani G (2015) The fate of silica based Stöber particles soaked into growth media (RPMI and M254): a DLS and ξ-potential study. Colloids Surf B: Biointerfaces. doi:10.1016/j.colsurfb.2015.03.033
22. Rahman IA, Vejayakumaran P, Sipaut CS, Ismail J, Chee CK (2008) Effect of the drying techniques on the morphology of silica nanoparticles synthesized via sol–gel process. Ceram Int 34:2059–2066
23. Hench LL, West JK (1990) The sol–gel process. Chem Rev 90:33–72
24. Brinker CJ, Scherer GW (1990) Sol–gel science: the physics and chemistry of sol–gel processing. Academic Press, San Diego
25. Stöber W, Fink A (1968) Controlled growth of monodisperse silica spheres in the micron size range. J Colloid Interface Sci 26:62–69
26. Illers KH (1980) Heat of fusion and specific volume of poly(-ethylene terephthalate) and poly(butylenes terephthalate. Colloid Polym Sci 258:117–123
27. Che J, Xiao Y, Luan B, Dong X, Wang X (2007) Surface structure, grafted chain length, and dispersion analysis of PBT prepolymer grafted nano-silica. J Mater Sci 42:4967–4975
28. Deshmukh GS, Peshwe DR, Pathak SU, Ekhe JD (2014) Non-isothermal crystallization kinetics and melting behavior of poly(butylene terephthalate) (PBT) composites based on different types of functional fillers. Thermochim Acta 581:41–53
29. Ohtsuki C, Kokubo T, Yamamuro T (1992) Mechanism of apatite formation on $CaO–SiO_2–P_2O_5$ glasses in a simulated body fluid. J Non-Cryst Solids 143:84–92
30. Kim CY, Clark AE, Hench LL (1989) Early stages of calcium-phosphate layer formation in bioglasses. J Non-Cryst Solids 113:195–202
31. Costantini A, Luciani G, Annunziata G, Silvestri B, Branda F (2006) Swelling properties and bioactivity of silica gel/pHEMA nanocomposites. J Mater Sci Mater Med 17:319–325
32. Bourara H, Hadjout S, Benabdelghani Z, Etxeberria A (2014) Miscibility and hydrogen bonding in blends of poly(4-vinylphenol)/poly(vinyl methyl ketone). Polymers 6:2752–2763
33. Kuo SW, Kao HC, Chang FC (2003) Thermal behavior and specific interaction in high glass transition temperature PMMA copolymer. Polymer 44:6873–6882
34. Pantelidou M, Chitnis PR, Breton J (2004) FTIR spectroscopy of synechocystis 6803 mutants affected on the hydrogen bonds to the carbonyl groups of the PsaA chlorophyll of P700 supports an extensive delocalization of the charge in P700. Biochemistry 43:8380–8390
35. Hobbs SY, Pratt CF (1975) Multiple melting in poly(butylene terephthalate). Polymer 16:462–464
36. Nichols ME, Robertson RE (1992) The multiple melting endotherms from poly (butylene terephthalate). J Polym Sci Pol Phys 30:755–768
37. Righetti MC, Di Lorenzo ML (2004) Melting process of poly (butylene terephthalate) analyzed by temperature-modulated differential scanning calorimetry. J Polym Sci Pol Phys 42: 2191–2201
38. Bula K, Jesionowski T, Krysztafkiewicz A, Janik J (2007) The effect of filler surface modification and processing conditions on distribution behaviour of silica nanofillers in polyesters. Colloid Polym Sci 285:1267–1273
39. Zhang X, Tian X, Zheng J, Yao X, Liu W, Cui P, Li Y (2008) Relationship between microstructure and tensile properties of PET/silica nanocomposite fibers. J Macromol Sci Phys 47: 368–377
40. Gashti MP, Hajiraissi R, Gashti MP (2013) Morphological, optical and electromagnetic characterization of polybutylene terephthalate/silica nanocomposites. Fibers Polym 14:1324–1331
41. Koti Reddy C, Shekharam T, Shailaja D (2012) Preparation and characterization of poly(chlorotrifluoroethylene-co-ethylvinyl ether)/poly(styrene acrylate) core-shells and SiO_2 nanocomposite films via a solution mixing method. J Appl Polym Sci 126: 1709–1713
42. Yao X, Tian X, Zhang X, Zheng K, Zheng J, Wang R, Kang S, Cui P (2009) Preparation and characterization of poly(butyleneterephthalate)/silica nanocomposites. Polym Eng Sci 4:799–807
43. Jiang Z, Siengchin S, Zhou LM, Steeg M, Karger-Kocsis J, Man HC (2009) Poly (butylene terephthalate)/silica nanocomposites prepared from cyclic butylene terephthalate. Compos Part A: Appl Sci Manuf 40:273–278